Task ID: 425.018
Task Title: Destruction of Perfluoroalkyl Surfactants in Semiconductor Process Waters Using Boron Doped Diamond Film Electrodes
Deliverable: Report on the susceptibility of a variety of PFAS compounds to electrolysis at BDD anodes and cathodes

Summary Abstract:

This research investigated oxidation of perfluroalkyl sulfonate (PFAS) including perfluorooctane sulfoate (PFOS) and perfluorobutane sulfonate (PFBS) using anodes composed of boron doped diamond (BDD) films on p-silicon substrates. Experiments measuring oxidation rates of PFOS and PFBS were performed over a range in current densities and temperatures using a rotating disk electrode (RDE) reactor and a parallel plate flow-through reactor. Both PFOS and PFBS oxidation produced carbon dioxide, sulfate, fluoride, and trace amounts of trifluoracetic acid (TFA). Production of TFA accounted for less than 3% of the PFOS or PFBS removed. Reaction rates in the RDE reactor were zeroth order in concentration, which is indicative of a reaction limited by the availability of reactive sites. Reaction rates in the flow-through reactor were mass transfer limited and were first order in concentration. Reaction rates measured as a function of temperature yielded an apparent activation energy consistent with an unactivated process. Density functional simulations were used to calculate the reaction energies and activation barriers for both PFOS and PFBS oxidation by hydroxyl radicals and by direct electron transfer. High activation barriers (i.e. PFBS: 123 ~ 288 kJ/mol; PFOS: 122 ~ 241 kJ/mol) for $HO^{\bullet}$ attack at different sites on the PFAS molecule indicated that oxidation by hydroxyl radicals was not the rate limiting mechanism for PFAS oxidation. Activation energies for direct electron transfer calculated as a function of the electrode potential indicated that the experiments were performed at sufficiently high overpotentials that the reactions could proceed via an activationless direct electron transfer mechanism.

Technical Results and Data:

Figure 1 shows PFOS concentrations as a function of electrolysis time for current densities ranging from 1 to 20 mA/cm^2 at a temperature of 22 °C. Reaction rates were zeroth order in PFOS concentration over the entire range of current densities. The zeroth order reaction kinetics can be attributed to reactive site saturation at the electrode surface. The reaction products recovered consisted of sulfate, fluoride, and trace levels of trifluoroacetic acid (TFA). Over the course of the experiments, solution pH values decreased from 4 to ~2.3**,** which is indicative of carbonic acid production. The trace amounts of TFA recovered represented less than 3% of the PFOS removed. One sulfate and an average of 11±0.5 fluoride ions were produced per PFOS oxidized. The recovery of only 11 out of 17 fluoride ions per PFOS removed indicates that there were losses of volatile compounds from the solution. These volatile compounds likely include TFA, HOF and possibly HF. Loss of hypofluorite from the solution was qualitatively indicated by the presence of a bleach-like odor.

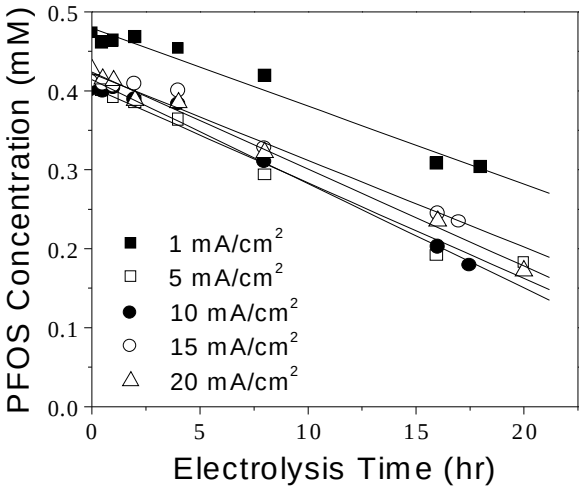

Figure 1: PFOS concentration as a function of electrolysis time at current density of 1(■), 5 (□), 10 (●), 15 (○) and 20 (Δ) m/cm^2 in a RDE reactor at 22 ℃.

To prevent the loss of volatile compounds, experiments were also performed in a gas-tight, flow-through reactor. Figure 2 shows the decline in PFOS concentrations as a function of the electrolysis time at a current density of 20 mA/cm^2 and 22 °C. PFOS reaction rates in the flow-through reactor were first order in concentration. The difference in reaction order between the flow-through and RDE experiments can be attributed to mass transfer limitations in the flow-through reactor. For example, the zeroth order rate constant measured using the RDE at a current density of 20 mA/cm^2 would result in complete PFOS removal after only 8 minutes.

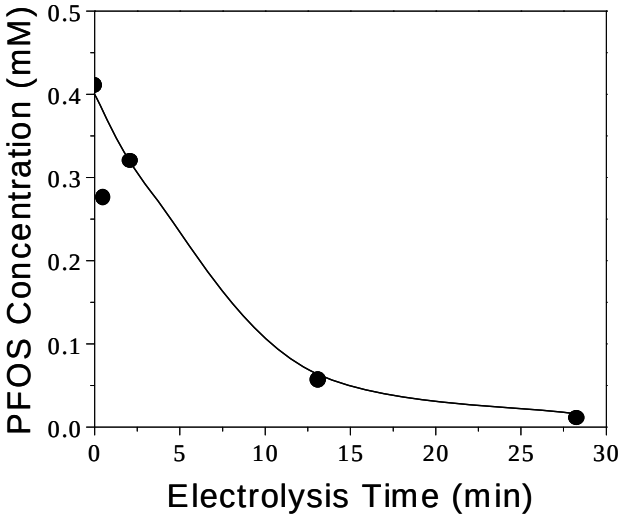

Figure 2: PFOS concentrations as a function of electrolysis time in the flow-through reactor operated at a current density of 20 mA/cm^2 at 22 ℃. The line represents first order model fits to the data.

The reaction products in the flow-through system were the same as those in the RDE reactor except for a greater fluoride mass balance. The fluoride mass balance increased to 14 out of 17 in the flow-through reactor. Only trace levels of TFA, representing less than 3% of the PFOS removed, were detected.

PFBS oxidation at BDD anode is quite similar to PFOS. Reaction rates were also zeroth order in PFBS concentration over the entire range of current densities in the RDE reactor and first order at lower concentration in the flow-through reactor. The major products include sulfate and fluoride ions. The only organic reaction product detected was trifluoroacetic acid (TFA), which appeared at trace levels representing <3% of the PFBS removed.

The temperature dependence of the PFAS reaction rates can be used to gain insight into the rate-limiting step in the reaction mechanism. PFBS reaction rates measured at 7, 15, 22, 25 and 45 °C were used to determine the apparent activation energies for PFBS oxidation, as illustrated in the Arrhenius plot shown in Figure 3. The data in Figure 3 yield an apparent activation energy of 9.3 ± 3 kJ/mol. Reactions with activation barriers this low generally proceed readily at room temperature (1). Arrhenius analysis of zeroth order rate constants at a fixed electrode potential yielded an apparent activation energy for PFOS oxidation of 4.2 kJ/mol.

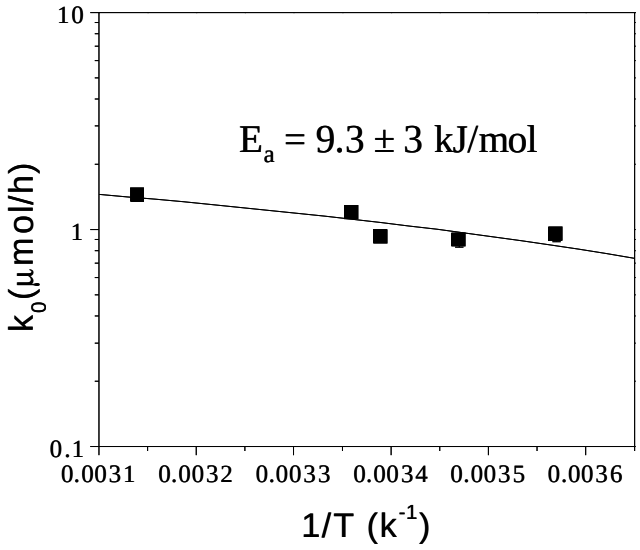

Figure 3: Arrhenius plot of zeroth order rate constants for PFBS oxidation at a fixed current density of 10 mA/cm^2.

DFT simulations were performed to determine the activation barriers for the reaction of hydroxyl radicals at different sites on the PFAS molecule. Figure 4 shows the transition state and final product for hydroxyl radical attack at the $-SO_3^-$ group. The reaction produced HSO_4^- and a nonafluoro-1-butane radical with an overall reaction energy of -84 kJ/mol. The activation energy determined from the transition state was 123 kJ/mol. Hydroxyl radical activation barriers this high are generally associated with reactions that do not readily occur at room temperature (1). For example, activation energies for $HO^\bullet$ reaction with perchlorinated biphenyls (PCBs) range from 71 to 93

kJ/mol (2, 3). This is consistent with the lack of PCB oxidation by hydroxyl radicals at room temperature. In contrast, phenol, which readily reacts with hydroxyl radicals, has activation barriers ranging from 4 to 25 kJ/mol, depending on the site of attack (4).

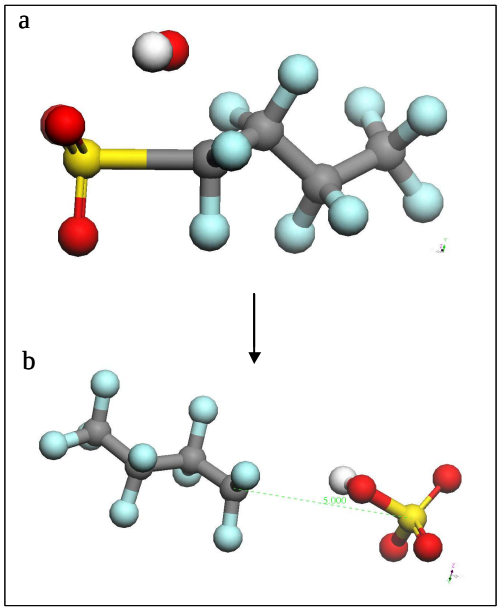

Figure 4: Transition state (a) and final products (b) for hydroxyl radical attack at the $-SO_3^-$ group.

DFT simulations were used to determine the activation energies for direct oxidation of PFBS as a function of the electrode potential using the methods described in Anderson and Kang (5). DFT simulations indicate that loss of one electron leads to lengthening of the C-S bond, and that the C-S bond length closely approximates the reaction coordinate (*i.e.*, >90% of the energy change between the reactant and the transition state is due to C-S bond lengthening). Figure 5a shows the energy of the reactant (PFBS anion) and products (PFBS neutral radical + electron) as a function of the C-S bond length at a potential of 2.5 V/SHE. Product energies as a function of electrode potential were determined by shifting the energy profile of the product species downwards by 106.1 kJ (*i.e.*, 1.0 eV) to increase the electrode potential by 1.0 V and upwards by 106.1 kJ to decrease the electrode potential by 1.0 V (5). Energies from the vacuum scale were converted to the SHE scale by subtracting 4.6 eV (5). The higher the electrode potential, the shorter the C-S bond stretching required for the reactant and product energy profiles to intersect. Intersection of the two energy profiles yields the bond length at the transition state and the activation energy for the reaction:

$$C_4F_9SO_3^- \rightarrow C_4F_9SO_3^{\bullet} + e^- \qquad (1)$$

By shifting the products energy profile up and down, activation energies as a function of electrode potential were calculated, as shown in Figure 5b. Figure 5b shows that the activation energy decreases from 270 kJ/mol at a potential of 1.0 V/SHE to zero at a potential of 3.0 V/SHE. This indicates that the reaction becomes activationless at

potentials greater than 3.0 V/SHE, and is consistent with the low apparent activation energy calculated in Figure 3.

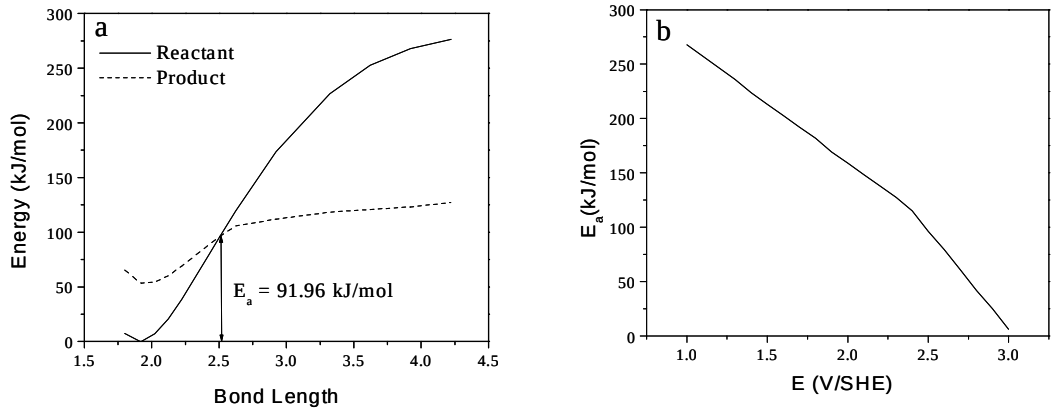

Figure 5: a) Energy profiles for reactant ($C_4F_9SO_3^-$) and products ($C_4F_9SO_3^\bullet + e^-$) for vertical electron transfer as a function of the C-S bond length at an electrode potential of 2.5 V/SHE. b) Activation energies as a function of electrode potential for a direct electron transfer reaction.

Density functional theory (DFT) simulations found that activation energies for hydroxyl radical oxidation of PFOS at different reaction sites ranged from 122 to 241 kJ/mol. These high activation barriers are consistent the lack of reactivity of PFOS with conventional hydrogen peroxide base advanced oxidation processes. DFT calculated activation barriers for direct oxidation of PFOS indicated that the reaction is activationless at electrode potentials higher than 2.7 V with respect to the standard hydrogen electrode (SHE). The low experimentally measured activation barrier and the calculated activationless electron transfer reaction at potentials above 2.7 V/SHE indicates that direct electron transfer is the rate limiting step for PFOS oxidation.

References

(*1*) Wade, L.G. Jr. *Organic Chemistry*, Prentice Hall, 4th edition, 1999.
(*2*) Murena, F. Schioppa, E.; Gioia, F., *Environ. Sci. Technol*. **2000**, 34, 4382-4385.
(*3)* Lin, Y. J.; Chen, Y. L.; Huang, C. Y.; Wu, M. F., *J. Hazard. Mater*. **2006**, 136, 902-910.
(*4*) Wang, Y.; Liu, Y.; Luo, Y.; Zhang, W.; Zhong, R.; *Acta Phys.-Chim. Sin*. 2006, 22, 1266-1271.
(*5*) Anderson, A. F.; Kang, D. B. *J. Phys. Chem. A*, **1998**, 102, 5993-5996.